

Study of the associated production of photons and b -quark jets in $p\bar{p}$ collisions at $\sqrt{s} = 1.96$ TeV

T. Aaltonen,²⁴ J. Adelman,¹⁴ B. Álvarez González,^{12,w} S. Amerio,^{44b,44a} D. Amidei,³⁵ A. Anastassov,³⁹ A. Annovi,²⁰ J. Antos,¹⁵ G. Apollinari,¹⁸ A. Apresyan,⁴⁹ T. Arisawa,⁵⁸ A. Artikov,¹⁶ J. Asaadi,⁵⁴ W. Ashmanskas,¹⁸ A. Attal,⁴ A. Aurisano,⁵⁴ F. Azfar,⁴³ W. Badgett,¹⁸ A. Barbaro-Galtieri,²⁹ V. E. Barnes,⁴⁹ B. A. Barnett,²⁶ P. Barria,^{47c,47a} P. Bartos,¹⁵ G. Bauer,³³ P.-H. Beauchemin,³⁴ F. Bedeschi,^{47a} D. Beecher,³¹ S. Behari,²⁶ G. Bellettini,^{47b,47a} J. Bellinger,⁶⁰ D. Benjamin,¹⁷ A. Beretvas,¹⁸ A. Bhatti,⁵¹ M. Binkley,¹⁸ D. Bisello,^{44b,44a} I. Bizjak,^{31,dd} R. E. Blair,² C. Blocker,⁷ B. Blumenfeld,²⁶ A. Bocci,¹⁷ A. Bodek,⁵⁰ V. Boisvert,⁵⁰ D. Bortoletto,⁴⁹ J. Boudreau,⁴⁸ A. Boveia,¹¹ B. Brau,^{11,b} A. Bridgeman,²⁵ L. Brigliadori,^{6b,6a} C. Bromberg,³⁶ E. Brubaker,¹⁴ J. Budagov,¹⁶ H. S. Budd,⁵⁰ S. Budd,²⁵ K. Burkett,¹⁸ G. Busetto,^{44b,44a} P. Bussey,²² A. Buzatu,³⁴ K. L. Byrum,² S. Cabrera,^{17,y} C. Calancha,³² S. Camarda,⁴ M. Campanelli,³¹ M. Campbell,³⁵ F. Canelli,^{14,18} A. Canepa,⁴⁶ B. Carls,²⁵ D. Carlsmith,⁶⁰ R. Carosi,^{47a} S. Carrillo,^{19,o} S. Carron,¹⁸ B. Casal,¹² M. Casarsa,¹⁸ A. Castro,^{6b,6a} P. Catastini,^{47c,47a} D. Cauz,^{55a} V. Cavaliere,^{47c,47a} M. Cavalli-Sforza,⁴ A. Cerri,²⁹ L. Cerrito,^{31,r} S. H. Chang,²⁸ Y. C. Chen,¹ M. Chertok,⁸ G. Chiarelli,^{47a} G. Chlachidze,¹⁸ F. Chlebana,¹⁸ K. Cho,²⁸ D. Chokheli,¹⁶ J. P. Chou,²³ K. Chung,^{18,p} W. H. Chung,⁶⁰ Y. S. Chung,⁵⁰ T. Chwalek,²⁷ C. I. Ciobanu,⁴⁵ M. A. Ciocci,^{47c,47a} A. Clark,²¹ D. Clark,⁷ G. Compostella,^{44a} M. E. Convery,¹⁸ J. Conway,⁸ M. Corbo,⁴⁵ M. Cordelli,²⁰ C. A. Cox,⁸ D. J. Cox,⁸ F. Crescioli,^{47b,47a} C. Cuenca Almenar,⁶¹ J. Cuevas,^{12,w} R. Culbertson,¹⁸ J. C. Cully,³⁵ D. Dagenhart,¹⁸ M. Datta,¹⁸ T. Davies,²² P. de Barbaro,⁵⁰ S. De Cecco,^{52a} A. Deisher,²⁹ G. De Lorenzo,⁴ M. Dell'Orso,^{47b,47a} C. Deluca,⁴ L. Demortier,⁵¹ J. Deng,^{17,g} M. Deninno,^{6a} M. d'Errico,^{44b,44a} A. Di Canto,^{47b,47a} G. P. di Giovanni,⁴⁵ B. Di Ruzza,^{47a} J. R. Dittmann,⁵ M. D'Onofrio,⁴ S. Donati,^{47b,47a} P. Dong,¹⁸ T. Dorigo,^{44a} S. Dube,⁵³ K. Ebina,⁵⁸ A. Elagin,⁵⁴ R. Erbacher,⁸ D. Errede,²⁵ S. Errede,²⁵ N. Ershaidat,^{45,cc} R. Eusebi,⁵⁴ H. C. Fang,²⁹ S. Farrington,⁴³ W. T. Fedorko,¹⁴ R. G. Feild,⁶¹ M. Feindt,²⁷ J. P. Fernandez,³² C. Ferrazza,^{47d,47a} R. Field,¹⁹ G. Flanagan,^{49,t} R. Forrest,⁸ M. J. Frank,⁵ M. Franklin,²³ J. C. Freeman,¹⁸ I. Furic,¹⁹ M. Gallinaro,⁵¹ J. Galyardt,¹³ F. Garberson,¹¹ J. E. Garcia,²¹ A. F. Garfinkel,⁴⁹ P. Garosi,^{47c,47a} H. Gerberich,²⁵ D. Gerdes,³⁵ A. Gessler,²⁷ S. Giagu,^{52b,52a} V. Giakoumopoulou,³ P. Giannetti,^{47a} K. Gibson,⁴⁸ J. L. Gimmell,⁵⁰ C. M. Ginsburg,¹⁸ N. Giokaris,³ M. Giordani,^{55b,55a} P. Giromini,²⁰ M. Giunta,^{47a} G. Giurgiu,²⁶ V. Glagolev,¹⁶ D. Glenzinski,¹⁸ M. Gold,³⁸ N. Goldschmidt,¹⁹ A. Golossanov,¹⁸ G. Gomez,¹² G. Gomez-Ceballos,³³ M. Goncharov,³³ O. González,³² I. Gorelov,³⁸ A. T. Goshaw,¹⁷ K. Goulianos,⁵¹ A. Gresele,^{44b,44a} S. Grinstein,⁴ C. Grosso-Pilcher,¹⁴ R. C. Group,¹⁸ U. Grundler,²⁵ J. Guimaraes da Costa,²³ Z. Gunay-Unalan,³⁶ C. Haber,²⁹ S. R. Hahn,¹⁸ E. Halkiadakis,⁵³ B.-Y. Han,⁵⁰ J. Y. Han,⁵⁰ F. Happacher,²⁰ K. Hara,⁵⁶ D. Hare,⁵³ M. Hare,⁵⁷ R. F. Harr,⁵⁹ M. Hartz,⁴⁸ K. Hatakeyama,⁵ C. Hays,⁴³ M. Heck,²⁷ J. Heinrich,⁴⁶ M. Herndon,⁶⁰ J. Heuser,²⁷ S. Hewamanage,⁵ D. Hidas,⁵³ C. S. Hill,^{11,d} D. Hirschbuehl,²⁷ A. Hocker,¹⁸ S. Hou,¹ M. Houlden,³⁰ S.-C. Hsu,²⁹ R. E. Hughes,⁴⁰ M. Hurwitz,¹⁴ U. Husemann,⁶¹ M. Hussein,³⁶ J. Huston,³⁶ J. Incandela,¹¹ G. Introzzi,^{47a} M. Iori,^{52b,52a} A. Ivanov,^{8,q} E. James,¹⁸ D. Jang,¹³ B. Jayatilaka,¹⁷ E. J. Jeon,²⁸ M. K. Jha,^{6a} S. Jindariani,¹⁸ W. Johnson,⁸ M. Jones,⁴⁹ K. K. Joo,²⁸ S. Y. Jun,¹³ J. E. Jung,²⁸ T. R. Junk,¹⁸ T. Kamon,⁵⁴ D. Kar,¹⁹ P. E. Karchin,⁵⁹ Y. Kato,^{42,n} R. Kephart,¹⁸ W. Ketchum,¹⁴ J. Keung,⁴⁶ V. Khotilovich,⁵⁴ B. Kilminster,¹⁸ D. H. Kim,²⁸ H. S. Kim,²⁸ H. W. Kim,²⁸ J. E. Kim,²⁸ M. J. Kim,²⁰ S. B. Kim,²⁸ S. H. Kim,⁵⁶ Y. K. Kim,¹⁴ N. Kimura,⁵⁸ L. Kirsch,⁷ S. Klimenko,¹⁹ K. Kondo,⁵⁸ D. J. Kong,²⁸ J. Konigsberg,¹⁹ A. Korytov,¹⁹ A. V. Kotwal,¹⁷ M. Kreps,²⁷ J. Kroll,⁴⁶ D. Krop,¹⁴ N. Krumnack,⁵ M. Kruse,¹⁷ V. Krutelyov,¹¹ T. Kuhr,²⁷ N. P. Kulkarni,⁵⁹ M. Kurata,⁵⁶ S. Kwang,¹⁴ A. T. Laasanen,⁴⁹ S. Lami,^{47a} S. Lammel,¹⁸ M. Lancaster,³¹ R. L. Lander,⁸ K. Lannon,^{40,v} A. Lath,⁵³ G. Latino,^{47c,47a} I. Lazzizzera,^{44b,44a} T. LeCompte,² E. Lee,⁵⁴ H. S. Lee,¹⁴ J. S. Lee,²⁸ S. W. Lee,^{54,x} S. Leone,^{47a} J. D. Lewis,¹⁸ C.-J. Lin,²⁹ J. Linacre,⁴³ M. Lindgren,¹⁸ E. Lipeles,⁴⁶ A. Lister,²¹ D. O. Litvintsev,¹⁸ C. Liu,⁴⁸ T. Liu,¹⁸ N. S. Lockyer,⁴⁶ A. Loginov,⁶¹ L. Lovas,¹⁵ D. Lucchesi,^{44b,44a} J. Lueck,²⁷ P. Lujan,²⁹ P. Lukens,¹⁸ G. Lungu,⁵¹ J. Lys,²⁹ R. Lysak,¹⁵ D. MacQueen,³⁴ R. Madrak,¹⁸ K. Maeshima,¹⁸ K. Makhoul,³³ P. Maksimovic,²⁶ S. Malde,⁴³ S. Malik,³¹ G. Manca,^{30,f} A. Manousakis-Katsikakis,³ F. Margaroli,⁴⁹ C. Marino,²⁷ C. P. Marino,²⁵ A. Martin,⁶¹ V. Martin,^{22,1} M. Martínez,⁴ R. Martínez-Ballarín,³² P. Mastrandrea,^{52a} M. Mathis,²⁶ M. E. Mattson,⁵⁹ P. Mazzanti,^{6a} K. S. McFarland,⁵⁰ P. McIntyre,⁵⁴ R. McNulty,^{30,k} A. Mehta,³⁰ P. Mehtala,²⁴ A. Menzione,^{47a} C. Mesropian,⁵¹ T. Miao,¹⁸ D. Mietlicki,³⁵ N. Miladinovic,⁷ R. Miller,³⁶ C. Mills,²³ M. Milnik,²⁷ A. Mitra,¹ G. Mitselmakher,¹⁹ H. Miyake,⁵⁶ S. Moed,²³ N. Moggi,^{6a} M. N. Mondragon,^{18,o} C. S. Moon,²⁸ R. Moore,¹⁸ M. J. Morello,^{47a} J. Morlock,²⁷ P. Movilla Fernandez,¹⁸ J. Mülmenstädt,²⁹ A. Mukherjee,¹⁸ Th. Muller,²⁷ P. Murat,¹⁸ M. Mussini,^{6b,6a} J. Nachtman,^{18,p} Y. Nagai,⁵⁶ J. Naganoma,⁵⁶ K. Nakamura,⁵⁶ I. Nakano,⁴¹ A. Napier,⁵⁷ J. Nett,⁶⁰ C. Neu,^{46,aa} M. S. Neubauer,²⁵ S. Neubauer,²⁷ J. Nielsen,^{29,h} L. Nodulman,² M. Norman,¹⁰ O. Norniella,²⁵ E. Nurse,³¹ L. Oakes,⁴³ S. H. Oh,¹⁷ Y. D. Oh,²⁸ I. Oksuzian,¹⁹ T. Okusawa,⁴² R. Orava,²⁴ K. Osterberg,²⁴ S. Pagan Griso,^{44b,44a} C. Pagliarone,^{55a} E. Palencia,¹⁸ V. Papadimitriou,¹⁸ A. Papaikonomou,²⁷ A. A. Paramanov,² B. Parks,⁴⁰ S. Pashapour,³⁴

J. Patrick,¹⁸ G. Pauletta,^{55b,55a} M. Paulini,¹³ C. Paus,³³ T. Peiffer,²⁷ D. E. Pellett,⁸ A. Penzo,^{55a} T. J. Phillips,¹⁷ G. Piacentino,^{47a} E. Pianori,⁴⁶ L. Pinera,¹⁹ K. Pitts,²⁵ C. Plager,⁹ L. Pondrom,⁶⁰ K. Potamianos,⁴⁹ O. Poukhov,^{16,a} F. Prokoshin,^{16,z} A. Pronko,¹⁸ F. Ptohos,^{18,j} E. Pueschel,¹³ G. Punzi,^{47b,47a} J. Pursley,⁶⁰ J. Rademacker,^{43,d} A. Rahaman,⁴⁸ V. Ramakrishnan,⁶⁰ N. Ranjan,⁴⁹ I. Redondo,³² P. Renton,⁴³ M. Renz,²⁷ M. Rescigno,^{52a} S. Richter,²⁷ F. Rimondi,^{6b,6a} L. Ristori,^{47a} A. Robson,²² T. Rodrigo,¹² T. Rodriguez,⁴⁶ E. Rogers,²⁵ S. Rolli,⁵⁷ R. Roser,¹⁸ M. Rossi,^{55a} R. Rossin,¹¹ P. Roy,³⁴ A. Ruiz,¹² J. Russ,¹³ V. Rusu,¹⁸ B. Rutherford,¹⁸ H. Saarikko,²⁴ A. Safonov,⁵⁴ W. K. Sakumoto,⁵⁰ L. Santi,^{55b,55a} L. Sartori,^{47a} K. Sato,⁵⁶ A. Savoy-Navarro,⁴⁵ P. Schlabach,¹⁸ A. Schmidt,²⁷ E. E. Schmidt,¹⁸ M. A. Schmidt,¹⁴ M. P. Schmidt,^{61,a} M. Schmitt,³⁹ T. Schwarz,⁸ L. Scodellaro,¹² A. Scribano,^{47c,47a} F. Scuri,^{47a} A. Sedov,⁴⁹ S. Seidel,³⁸ Y. Seiya,⁴² A. Semenov,¹⁶ L. Sexton-Kennedy,¹⁸ F. Sforza,^{47b,47a} A. Sfyrila,²⁵ S. Z. Shalhout,⁵⁹ T. Shears,³⁰ P. F. Shepard,⁴⁸ M. Shimojima,^{56,u} S. Shiraishi,¹⁴ M. Shochet,¹⁴ Y. Shon,⁶⁰ I. Shreyber,³⁷ A. Simonenko,¹⁶ P. Sinervo,³⁴ A. Sisakyan,¹⁶ A. J. Slaughter,¹⁸ J. Slaunwhite,⁴⁰ K. Sliwa,⁵⁷ J. R. Smith,⁸ F. D. Snider,¹⁸ R. Snihur,³⁴ A. Soha,¹⁸ S. Somalwar,⁵³ V. Sorin,⁴ P. Squillacioti,^{47c,47a} M. Stanitzki,⁶¹ R. St. Denis,²² B. Stelzer,³⁴ O. Stelzer-Chilton,³⁴ D. Stentz,³⁹ J. Strologas,³⁸ G. L. Strycker,³⁵ J. S. Suh,²⁸ A. Sukhanov,¹⁹ I. Suslov,¹⁶ A. Taffard,^{25,g} R. Takashima,⁴¹ Y. Takeuchi,⁵⁶ R. Tanaka,⁴¹ J. Tang,¹⁴ M. Tecchio,³⁵ P. K. Teng,¹ J. Thom,^{18,i} J. Thome,¹³ G. A. Thompson,²⁵ E. Thomson,⁴⁶ P. Tipton,⁶¹ P. Ttito-Guzmán,³² S. Tkaczyk,¹⁸ D. Toback,⁵⁴ S. Tokar,¹⁵ K. Tollefson,³⁶ T. Tomura,⁵⁶ D. Tonelli,¹⁸ S. Torre,²⁰ D. Torretta,¹⁸ P. Totaro,^{55b,55a} S. Tourneur,⁴⁵ M. Trovato,^{47d,47a} S.-Y. Tsai,¹ Y. Tu,⁴⁶ N. Turini,^{47c,47a} F. Ukegawa,⁵⁶ S. Uozumi,²⁸ N. van Remortel,^{24,c} A. Varganov,³⁵ E. Vataga,^{47d,47a} F. Vázquez,^{19,o} G. Velez,¹⁸ C. Vellidis,³ M. Vidal,³² I. Vila,¹² R. Vilar,¹² M. Vogel,³⁸ I. Volobouev,^{29,x} G. Volpi,^{47b,47a} P. Wagner,⁴⁶ R. G. Wagner,² R. L. Wagner,¹⁸ W. Wagner,^{27,bb} J. Wagner-Kuhr,²⁷ T. Wakisaka,⁴² R. Wallny,⁹ S. M. Wang,¹ A. Warburton,³⁴ D. Waters,³¹ M. Weinberger,⁵⁴ J. Weinelt,²⁷ W. C. Wester III,¹⁸ B. Whitehouse,⁵⁷ D. Whiteson,^{46,g} A. B. Wicklund,² E. Wicklund,¹⁸ S. Wilbur,¹⁴ G. Williams,³⁴ H. H. Williams,⁴⁶ P. Wilson,¹⁸ B. L. Winer,⁴⁰ P. Wittich,^{18,i} S. Wolbers,¹⁸ C. Wolfe,¹⁴ H. Wolfe,⁴⁰ T. Wright,³⁵ X. Wu,²¹ F. Würthwein,¹⁰ A. Yagil,¹⁰ K. Yamamoto,⁴² J. Yamaoka,¹⁷ U. K. Yang,^{14,s} Y. C. Yang,²⁸ W. M. Yao,²⁹ G. P. Yeh,¹⁸ K. Yi,^{18,p} J. Yoh,¹⁸ K. Yorita,⁵⁸ T. Yoshida,^{42,m} G. B. Yu,¹⁷ I. Yu,²⁸ S. S. Yu,¹⁸ J. C. Yun,¹⁸ A. Zanetti,^{55a} Y. Zeng,¹⁷ X. Zhang,²⁵ Y. Zheng,^{9,e} and S. Zucchelli^{6b,6a}

(CDF Collaboration)

¹*Institute of Physics, Academia Sinica, Taipei, Taiwan 11529, Republic of China*²*Argonne National Laboratory, Argonne, Illinois 60439, USA*³*University of Athens, 157 71 Athens, Greece*⁴*Institut de Física d'Altes Energies, Universitat Autònoma de Barcelona, E-08193, Bellaterra (Barcelona), Spain*⁵*Baylor University, Waco, Texas 76798, USA*^{6a}*Istituto Nazionale di Fisica Nucleare Bologna, I-40127 Bologna, Italy*^{6b}*University of Bologna, I-40127 Bologna, Italy*⁷*Brandeis University, Waltham, Massachusetts 02254, USA*⁸*University of California, Davis, Davis, California 95616, USA*⁹*University of California, Los Angeles, Los Angeles, California 90024, USA*¹⁰*University of California, San Diego, La Jolla, California 92093, USA*¹¹*University of California, Santa Barbara, Santa Barbara, California 93106, USA*¹²*Instituto de Física de Cantabria, CSIC-University of Cantabria, 39005 Santander, Spain*¹³*Carnegie Mellon University, Pittsburgh, Pennsylvania 15213, USA*¹⁴*Enrico Fermi Institute, University of Chicago, Chicago, Illinois 60637, USA*¹⁵*Comenius University, 842 48 Bratislava, Slovakia; Institute of Experimental Physics, 040 01 Kosice, Slovakia*¹⁶*Joint Institute for Nuclear Research, RU-141980 Dubna, Russia*¹⁷*Duke University, Durham, North Carolina 27708, USA*¹⁸*Fermi National Accelerator Laboratory, Batavia, Illinois 60510, USA*¹⁹*University of Florida, Gainesville, Florida 32611, USA*²⁰*Laboratori Nazionali di Frascati, Istituto Nazionale di Fisica Nucleare, I-00044 Frascati, Italy*²¹*University of Geneva, CH-1211 Geneva 4, Switzerland*²²*Glasgow University, Glasgow G12 8QQ, United Kingdom*²³*Harvard University, Cambridge, Massachusetts 02138, USA*²⁴*Division of High Energy Physics, Department of Physics, University of Helsinki and Helsinki Institute of Physics, FIN-00014, Helsinki, Finland*²⁵*University of Illinois, Urbana, Illinois 61801, USA*²⁶*The Johns Hopkins University, Baltimore, Maryland 21218, USA*²⁷*Institut für Experimentelle Kernphysik, Karlsruhe Institute of Technology, D-76131 Karlsruhe, Germany*

- ²⁸*Center for High Energy Physics: Kyungpook National University, Daegu 702-701, Korea; Seoul National University, Seoul 151-742, Korea; Sungkyunkwan University, Suwon 440-746, Korea; Korea Institute of Science and Technology Information, Daejeon 305-806, Korea; Chonnam National University, Gwangju 500-757, Korea; Chonbuk National University, Jeonju 561-756, Korea*
- ²⁹*Ernest Orlando Lawrence Berkeley National Laboratory, Berkeley, California 94720, USA*
- ³⁰*University of Liverpool, Liverpool L69 7ZE, United Kingdom*
- ³¹*University College London, London WC1E 6BT, United Kingdom*
- ³²*Centro de Investigaciones Energeticas Medioambientales y Tecnologicas, E-28040 Madrid, Spain*
- ³³*Massachusetts Institute of Technology, Cambridge, Massachusetts 02139, USA*
- ³⁴*Institute of Particle Physics: McGill University, Montréal, Québec, Canada H3A 2T8; Simon Fraser University, Burnaby, British Columbia, Canada V5A 1S6; University of Toronto, Toronto, Ontario, Canada M5S 1A7; and TRIUMF, Vancouver, British Columbia, Canada V6T 2A3*
- ³⁵*University of Michigan, Ann Arbor, Michigan 48109, USA*
- ³⁶*Michigan State University, East Lansing, Michigan 48824, USA*
- ³⁷*Institution for Theoretical and Experimental Physics, ITEP, Moscow 117259, Russia*
- ³⁸*University of New Mexico, Albuquerque, New Mexico 87131, USA*
- ³⁹*Northwestern University, Evanston, Illinois 60208, USA*
- ⁴⁰*The Ohio State University, Columbus, Ohio 43210, USA*
- ⁴¹*Okayama University, Okayama 700-8530, Japan*
- ⁴²*Osaka City University, Osaka 588, Japan*
- ⁴³*University of Oxford, Oxford OX1 3RH, United Kingdom*
- ^{44a}*Istituto Nazionale di Fisica Nucleare, Sezione di Padova-Trento, I-35131 Padova, Italy*
- ^{44b}*University of Padova, I-35131 Padova, Italy*
- ⁴⁵*LPNHE, Universite Pierre et Marie Curie/IN2P3-CNRS, UMR7585, Paris, F-75252 France*
- ⁴⁶*University of Pennsylvania, Philadelphia, Pennsylvania 19104, USA*
- ^{47a}*Istituto Nazionale di Fisica Nucleare Pisa, I-56127 Pisa, Italy*
- ^{47b}*University of Pisa, I-56127 Pisa, Italy*
- ^{47c}*University of Siena, I-56127 Pisa, Italy*
- ^{47d}*Scuola Normale Superiore, I-56127 Pisa, Italy*
- ⁴⁸*University of Pittsburgh, Pittsburgh, Pennsylvania 15260, USA*
- ⁴⁹*Purdue University, West Lafayette, Indiana 47907, USA*
- ⁵⁰*University of Rochester, Rochester, New York 14627, USA*
- ⁵¹*The Rockefeller University, New York, New York 10021, USA*

^aDeceased.

^bVisitor from University of Massachusetts Amherst, Amherst, MA 01003, USA.

^cVisitor from Universiteit Antwerpen, B-2610 Antwerp, Belgium.

^dVisitor from University of Bristol, Bristol BS8 1TL, United Kingdom.

^eVisitor from Chinese Academy of Sciences, Beijing 100864, China.

^fVisitor from Istituto Nazionale di Fisica Nucleare, Sezione di Cagliari, 09042 Monserrato (Cagliari), Italy.

^gVisitor from University of California Irvine, Irvine, CA 92697, USA.

^hVisitor from University of California Santa Cruz, Santa Cruz, CA 95064, USA.

ⁱVisitor from Cornell University, Ithaca, NY 14853, USA.

^jVisitor from University of Cyprus, Nicosia CY-1678, Cyprus.

^kVisitor from University College Dublin, Dublin 4, Ireland.

^lVisitor from University of Edinburgh, Edinburgh EH9 3JZ, United Kingdom.

^mVisitor from University of Fukui, Fukui City, Fukui Prefecture, Japan 910-0017.

ⁿVisitor from Kinki University, HigashiOsaka City, Japan 577-8502.

^oVisitor from Universidad Iberoamericana, Mexico D.F., Mexico.

^pVisitor from University of Iowa, Iowa City, IA 52242, USA.

^qVisitor from Kansas State University, Manhattan, KS 66506, USA.

^rVisitor from Queen Mary, University of London, London, E1 4NS, United Kingdom.

^sVisitor from University of Manchester, Manchester M13 9PL, United Kingdom.

^tVisitor from Muons, Inc., Batavia, IL 60510, USA.

^uVisitor from Nagasaki Institute of Applied Science, Nagasaki, Japan.

^vVisitor from University of Notre Dame, Notre Dame, IN 46556, USA.

^wVisitor from University de Oviedo, E-33007 Oviedo, Spain.

^xVisitor from Texas Tech University, Lubbock, TX 79609, USA.

^yVisitor from IFIC (CSIC-Universitat de Valencia), 56071 Valencia, Spain.

^zVisitor from Universidad Tecnica Federico Santa Maria, 110v Valparaiso, Chile.

^{aa}Visitor from University of Virginia, Charlottesville, VA 22906, USA.

^{bb}Visitor from Bergische Universität Wuppertal, 42097 Wuppertal, Germany.

^{cc}Visitor from Yarmouk University, Irbid 211-63, Jordan.

^{dd}On leave from J. Stefan Institute, Ljubljana, Slovenia.

^{52a}*Istituto Nazionale di Fisica Nucleare, Sezione di Roma 1, I-00185 Roma, Italy*^{52b}*Sapienza Università di Roma, I-00185 Roma, Italy*⁵³*Rutgers University, Piscataway, New Jersey 08855, USA*⁵⁴*Texas A&M University, College Station, Texas 77843, USA*^{55a}*Istituto Nazionale di Fisica Nucleare Trieste/Udine, I-34100 Trieste, Italy*^{55b}*University of Trieste/Udine, I-33100 Udine, Italy*⁵⁶*University of Tsukuba, Tsukuba, Ibaraki 305, Japan*⁵⁷*Tufts University, Medford, Massachusetts 02155, USA*⁵⁸*Waseda University, Tokyo 169, Japan*⁵⁹*Wayne State University, Detroit, Michigan 48201, USA*⁶⁰*University of Wisconsin, Madison, Wisconsin 53706, USA*⁶¹*Yale University, New Haven, Connecticut 06520, USA*

(Received 17 December 2009; published 15 March 2010)

The cross section for photon production in association with at least one jet containing a b quark has been measured in proton antiproton collisions at $\sqrt{s} = 1.96$ TeV. The data sample used corresponds to an integrated luminosity of 340 pb^{-1} collected with the CDF II detector. Both the differential cross section as a function of photon transverse energy E_T^γ and the total cross section are measured and compared to a next-to-leading order prediction for the process.

DOI: 10.1103/PhysRevD.81.052006

PACS numbers: 12.38.Qk, 13.85.Qk, 13.87.Ce

The study of final states with an isolated high energy photon and an identified b -quark jet is a testing ground for quantum chromodynamics (QCD) predictions at the Tevatron. At photon transverse energies E_T^γ below 70 GeV Compton scattering processes $gb \rightarrow \gamma gb$ or $qb \rightarrow \gamma qb$ dominate production, while above that value the dominant process is quark annihilation $q\bar{q} \rightarrow b\bar{b}\gamma$ [1]. A cross section measurement provides a probe of the hard scattering dynamics within the proton, and a cross-check of the predictions of its b -quark content, whose parton density function is indirectly extracted from constraints on the gluon density functions.

The first measurement of photon and heavy flavor jets (identified by the presence of a muon in the jet) was performed on 86 pb^{-1} of integrated luminosity taken at $\sqrt{s} = 1.8$ TeV with the CDF I detector [2]. The results were interpreted as limits to new physics involving decays of techni-omega states [3], or supersymmetric particles [4]. Recently the D0 Collaboration has measured the cross section of heavy flavor jets and photons [5] using data collected at $\sqrt{s} = 1.96$ TeV. In this paper we exploit the improved CDF II detector to identify b jets by a lifetime based secondary vertex tag, use a larger data set collected at a somehow higher energy probe, explore lower photon transverse energies, and employ a superior analysis technique where all backgrounds are determined from data.

The CDF II detector is described in detail in [6]. It is composed of a central spectrometer inside a 1.4 T magnetic field, surrounded by electromagnetic and hadronic calorimetry and muon chambers. The inner spectrometer measures charged particle trajectories with a transverse momentum (p_T) precision of $\Delta p_T/p_T^2 = 0.07\%(\text{GeV}/c)^{-1}$, and an uncertainty on the transverse impact parameter of about $40 \mu\text{m}$ for tracks of p_T above $1 \text{ GeV}/c$, which includes the intrinsic beam size of about $30 \mu\text{m}$. Information from the central tracker can be sent to the

hardware tracker silicon vertex tracker (SVT) [7] that compares hits from the tracking detectors with prefitted tracks stored in an associative memory to extract their parameters. An impact parameter resolution less than $50 \mu\text{m}$, including the contribution from the beam, can be obtained in time to be used at the trigger level. Central calorimeters [8] cover the region $|\eta| < 1.1$, with an electromagnetic (hadronic) energy resolution of $\sigma(E)/E = 13.5\%/\sqrt{E} \oplus 2.0\%$ ($\sigma(E)/E = 50\%/\sqrt{E_T} \oplus 3\%$). The end-wall hadronic calorimeter extends this coverage to $|\eta| < 1.3$ [9] with an energy resolution of $75\%/\sqrt{E_T} \oplus 4\%$, while the region $1.3 < |\eta| < 3.6$ is covered by forward calorimeters [10], with hadronic and electromagnetic energy resolutions of $80\%/\sqrt{E} \oplus 5\%$ and $16\%/\sqrt{E} \oplus 1\%$, respectively.

To distinguish electromagnetic clusters from photons, electrons, and decays of neutral pions, the central electromagnetic calorimeter is equipped with a preshower detector (CPR) in front of the calorimeter to detect early photon conversions in the solenoid coil, and a shower maximum detector (CES) placed inside the calorimeter to measure the shower profile. For each electromagnetic cluster a weight related to its probability of being a photon is given by comparing signals from these detectors to the expected shapes.

We use data obtained by two triggers: one which requires a photonlike object with transverse energy larger than 25 GeV (“high E_T^γ photon”), and one (“SVT photon”) which requires a photonlike object with transverse energy larger than 12 GeV, a jet with transverse energy larger than 10 GeV, and a track, measured by the SVT [7], with transverse momentum larger than $2 \text{ GeV}/c$, and an impact parameter larger than $120 \mu\text{m}$.

An integrated luminosity of $340 (208) \text{ pb}^{-1}$ of data was analyzed in the high E_T^γ photon (SVT photon) triggered data set.

The high E_T^γ photon trigger has an efficiency close to 100% for events with E_T^γ above 28 GeV, while the SVT photon trigger has an efficiency of $(50 \pm 4)\%$ (estimated from data, in the overlap region with the E_T^γ data set), for photons down to 12 GeV.

Selected events must pass at least one of the two photon triggers, contain an isolated central ($|\eta| < 1.1$) photon of $E_T^\gamma > 20$ GeV, and a b jet of $E_T > 20$ GeV within $|\eta| < 1.5$.

Photon candidates must have a calorimeter cluster with hadronic energy fraction smaller than $0.055 + 0.00045 * E^\gamma$, where E^γ is the photon energy. The shower profile must also agree with that expected for an electromagnetic deposit. In order to reduce contamination from neutral mesons, photon candidates must be isolated from nearby calorimeter deposits and tracks. We require that the total transverse energy deposits for clusters in a cone of radius $R = \sqrt{\Delta\phi^2 + \Delta\eta^2} = 0.4$ around the photon candidate are smaller than $2.0 + 0.02(E_T^\gamma - 20)$, and the same quantity for tracks must be smaller than $< 2.0 + E_T^\gamma * 0.005$ to ensure isolation in the tracking detectors. Events containing adjacent calorimeter clusters in the CES are rejected.

Jets are reconstructed using the JETCLU algorithm [11] with a cone radius 0.4 (0.7) for events containing photons of $E_T^\gamma < (>) 26$ GeV. To recover the true hadronic energy, jets are corrected for instrumental effects [12]. We select events containing at least one jet with $E_T > 20$ GeV, with $\Delta R > 0.7$ to the photon candidate. Jets originating from b hadrons are identified from displaced secondary vertices [13]. The secondary vertex must be more than 2 standard deviations away from the beam position, in the same direction as the jet momentum. At least one b jet must be identified for each event. The efficiency of the b -tagging algorithm is 25% for b jets of $E_T = 20$ GeV, increasing to 40% at $E_T = 50$ GeV.

The PYTHIA [14] Monte Carlo code is used to estimate the photon and jet selection efficiencies, using a Q^2 scale of the interaction of 225 GeV², and the CTEQ5L [15] parton distribution functions. A simulation of the underlying event is included [16]. Backgrounds to photons from high energy π^0 's, decaying to pairs of overlapping photons that cannot be distinguished, were estimated from data, using the signals from the CPR and CES detectors, following the procedure detailed in [17]. The fraction of correctly identified photons in the sample passing those selection criteria increases with E_T , going from about 50% at the lower end of the spectrum considered here (20 GeV) to around 80% at high E_T^γ . Backgrounds to b jets can arise from c -quark jets (charm hadrons have a lifetime between a quarter and two-thirds that of b hadrons), and light-quark jets where random combinations of tracks mimic a displaced vertex. The purity of the selected sample is determined from fitting the invariant mass of tracks composing the secondary vertex using Monte Carlo templates of the

shapes expected for b -, charm (c -), and light-quark jets. Figure 1 shows an example of the fit to the data. Here, about one-third of jets arise from b quarks. This invariant mass is lower than the corresponding hadron mass due to misassigned tracks and unreconstructed neutral hadrons, but template shapes of the different quark jet types are sufficiently different to provide reasonable discriminating power.

To estimate the b purity of the fake photon candidates, we assume that the composition of the tagged jet sample in π^0 + tagged jet events is similar to π^\pm + tagged jet events, so we use di-jet data. Events are required to contain two jets, one of which must be tagged and have similar transverse energy and pseudorapidity requirements to the b jet, and a second which passes similar kinematic requirements to the photon in our analysis. The fraction of b jets in this sample can be found by fitting the invariant mass at the secondary vertex of the tagged jets. The purity of the selected jets ranges from 50% for jets of E_T around 20 GeV, to about 15% for jets of E_T around 75 GeV, where the rate of light-quark jet tagging increases. This b fraction is then normalized to the estimated number of misidentified photons, and subtracted from the estimated number of b jets in the whole event sample.

Some 10 900 (55 800) events pass the selection criteria in the high transverse energy photon (SVT photon) triggered data sets. Candidate events are divided into bins of photon transverse energy. The numbers of events in each bin are corrected for background, trigger, selection, and acceptance efficiency, and divided by the appropriate integrated luminosity. The results are given in Table I, which also lists the systematic uncertainties detailed later. The statistical uncertainty for the high E_T^γ photon data set includes contributions from finite Monte Carlo statistics.

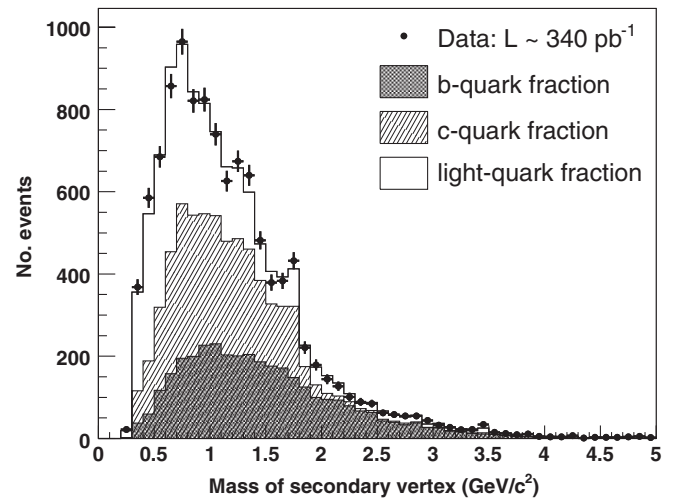


FIG. 1. Fit to the invariant mass of tracks composing the secondary vertex, for photon candidates having $E_T > 26$ GeV. The points are data, and the stacked, shaded histograms represent the estimated contributions of the b -, c -, and light-quark jets.

TABLE I. The measured differential cross section for central photon production in association with at least one b jet of $E_T > 20$ GeV, inside $|\eta| < 1.5$, tabulated as a function of the photon transverse energy E_T^γ . The first column is the energy range of each bin, the second is the measured cross section from data, and the third the prediction from NLO Monte Carlo. In data, the first (second) uncertainty quoted is statistical (systematic). For the Monte Carlo prediction the quoted uncertainty arises from the convolution of scale variation, parton distribution functions, and the numerical integration procedure [1]. Note that the first two measurements are made using the SVT data set, and the remainder with the high E_T^γ data set. Systematics about luminosity, the secondary vertex tagging scale factor, and the effect of multiple vertices are correlated between all bins. The uncertainty due to the statistical precision of the SVT trigger efficiency is only fully correlated between the first two bins only. All other uncertainties are uncorrelated between bins.

E_T^γ (GeV)	$d\sigma(p\bar{p} \rightarrow \gamma + \geq 1b \text{ jet})/dE_T^\gamma$ (pb/GeV)	$d\sigma(p\bar{p} \rightarrow \gamma + \geq 1b \text{ jet})/dE_T^\gamma$ (pb/GeV)
20–24	$3.90 \pm 0.49 \pm 0.84$	3.27 ± 0.78
24–28	$3.01 \pm 0.41 \pm 0.63$	3.67 ± 0.32
26–28 ^a	$3.13 \pm 0.51 \pm 0.67$	3.01 ± 0.21
28–31	$2.90 \pm 0.42 \pm 0.61$	2.65 ± 0.18
31–35	$1.24 \pm 0.20 \pm 0.27$	1.72 ± 0.14
35–43	$0.94 \pm 0.14^{+0.18}_{-0.20}$	0.92 ± 0.10
43–70	$0.20 \pm 0.03 \pm 0.04$	0.21 ± 0.05

^aThe overlap bin, is not used in the final results.

Sources of systematic uncertainty studied are photon identification, jet energy scale, b -jet identification, and luminosity. In the following only the largest contributions will be quantified.

The variables used in photon identification have been validated by comparing data and simulation in $Z \rightarrow e^+e^-$ decays [18], showing good agreement. Uncertainties in the fake photon estimate arise from assumed values of the hit rate in the preshower detector, backscattered showers rate, and the composition of fake photon backgrounds. The associated systematic uncertainty is about 6%.

The uncertainty on the jet energy scale has been studied in detail elsewhere [12] and the findings applied to this analysis. It decreases with increasing jet E_T , being about 5% for jets of 35 GeV E_T . Uncertainties have also been determined for multiple interactions overlapping in the same event, and the uncertainty on the b -jet scale. Uncertainties in the b -quark purity arise from imperfect modeling of the Monte Carlo template shapes. Differences in shape can arise between the secondary vertex invariant mass of jets containing one or two b quarks, or if track efficiency is incorrectly modeled. For the first effect we fit the data to templates composed of mixtures of single and double quark templates (ranging from 0% to 100%), and the χ^2 of the resulting distributions with respect to the default is computed. We take as a $1 - \sigma$ deviation the value for this mixture for which the χ^2 increases by one unit with respect to its minimum, and recalculate the cross section using this mixed template. The systematic uncertainty is the difference between this value and the cross section obtained with the default diquark fraction. This is the largest single source of uncertainty and is about 17%. Previous studies [19] suggest a difference in tracking efficiency between data and simulation which is a function of isolation, momentum, and position in the detector. We remake the invariant mass templates incorporating the

inefficiency derived from data, and take the full difference (5%) as a systematic uncertainty.

Other systematic uncertainties on b -jet identification arise from the difference in tagging efficiency between data and simulation, between single and double b jets, and from b hadron multiplicity. The difference in scale between tagging efficiency in data and simulation was found in [13] to be 0.91 ± 0.06 . This results in a 6% uncertainty on the measured cross sections. The uncertainty on tagging efficiency for single and double b jets is determined as the difference between results obtained using the fractions of single and double quark templates corresponding to ± 1 standard deviation, as found earlier, and is about 7%. We have adopted the findings of previous studies [19] of the effect of assumed b hadron multiplicity (a 1% effect on the measured cross section). The SVT-based analysis is also affected by the statistical precision of the trigger efficiency determination (about 10%). Finally, the luminosity is subject to a $\pm 6\%$ uncertainty [20].

The cross section for photons produced in association with b jets is tabulated in Table I, separately for the two data sets. There is overlap in the high- E_T range between the two data sets, and due to its greater statistical precision, the inclusive photon one is used in the final results. The measurements are corrected to the hadron level so that they can be directly compared to a next-to-leading order (NLO) calculation [1]. This prediction was derived analytically, using the CTEQ6.6M parton density functions [21], and a renormalization, factorization, and fragmentation scale set to the transverse momentum of the photon. It does not include nonperturbative effects (hadronization and underlying event), and is presented in terms of parton level jets.

The measured cross sections are compared with this prediction in Fig. 2. Also shown are the theoretical uncertainties due to choice of scale and uncertainty in parton density functions. Agreement with next-to-leading order is

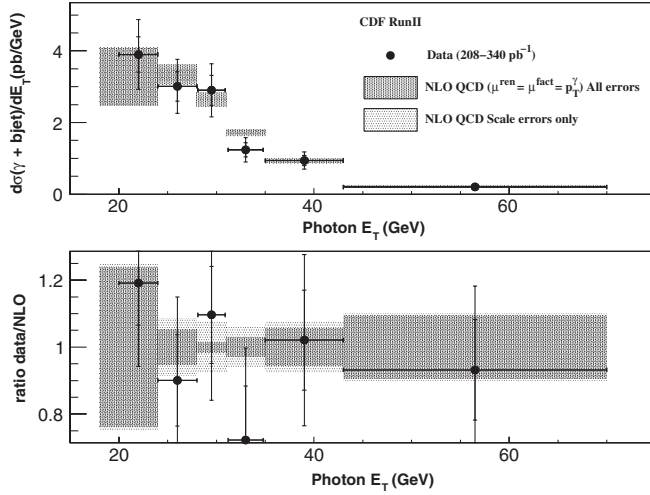


FIG. 2. Top panel: b + photon cross section as a function of photon E_T , compared to NLO QCD calculations. The light dashed is a quadrature sum of uncertainties coming from scale variation (both renormalization and factorization scales varied by a factor 2 and 0.5) and parton density functions, while the darker dashed represents the scale variation contribution only. The inner error bars for data represent the statistical uncertainties, the outer the combination of statistical and systematic. The bottom panel shows the ratio of data to the NLO calculation, where the error bars and shading have the same meaning as before.

good over the entire photon E_T^γ range probed. It should be noted that due to numerical stability problems, the first bin in the NLO calculation starts at 18 GeV instead of 20 as for the data.

The total cross section $\sigma(p\bar{p} \rightarrow \gamma + \geq 1b \text{ jet}; E_T^\gamma > 20 \text{ GeV})$ has been measured to be $54.22 \pm 3.26(\text{stat})^{+5.04}_{-5.09} \times (\text{syst}) \text{ pb}$. This is consistent with the next-to-leading order prediction of $55.62 \pm 3.87 \text{ pb}$.

In summary, the cross section for photon production in association with b jets has been measured in proton anti-proton collisions at $\sqrt{s} = 1.96 \text{ TeV}$ with the CDF II detector. The measurement has been made for b jets with $E_T > 20 \text{ GeV}$ inside $|\eta| < 1.5$, and for photons of at least $E_T^\gamma > 20 \text{ GeV}$ inside $|\eta| < 1.1$, including the lowest photon transverse energies probed to date. The results are consistent with next-to-leading order perturbative QCD predictions, using CTEQ6.6M parton density functions, throughout the photon E_T^γ range measured, while leading-order calculations would predict a cross section smaller by about 30%. The level of accuracy of this measurement is therefore already sufficient to discriminate between the first orders of perturbative expansion and favor the most precise NLO predictions.

We thank the Fermilab staff and the technical staffs of the participating institutions for their vital contributions. This work was supported by the U.S. Department of Energy and National Science Foundation; the Italian Istituto Nazionale di Fisica Nucleare; the Ministry of Education, Culture, Sports, Science and Technology of Japan; the Natural Sciences and Engineering Research Council of Canada; the National Science Council of the Republic of China; the Swiss National Science Foundation; the A.P. Sloan Foundation; the Bundesministerium für Bildung und Forschung, Germany; the World Class University Program, the National Research Foundation of Korea; the Science and Technology Facilities Council and the Royal Society, UK; the Institut National de Physique Nucleaire et Physique des Particules/CNRS; the Russian Foundation for Basic Research; the Ministerio de Ciencia e Innovación, and Programa Consolider-Ingenio 2010, Spain; the Slovak R&D Agency; and the Academy of Finland.

-
- [1] T. Stavreva and J. Owens, Phys. Rev. D **79**, 054017 (2009), and private communication.
 - [2] T. Affolder *et al.* (CDF Collaboration), Phys. Rev. D **65**, 052006 (2002).
 - [3] F. Abe *et al.* (CDF Collaboration), Phys. Rev. D **60**, 092003 (1999).
 - [4] T. Affolder *et al.* (CDF Collaboration), Phys. Rev. D **65**, 052006 (2002).
 - [5] V.M. Abazov *et al.* (D0 Collaboration), Phys. Rev. Lett. **102**, 192002 (2009).
 - [6] R. Blair *et al.* (CDF Collaboration), Report No. FERMILAB-PUB-96/390-E, 1996; D. Acosta *et al.* (CDF Collaboration), Phys. Rev. D **68**, 072004 (2003).
 - [7] W. Ashmanskas *et al.*, Nucl. Instrum. Methods Phys. Res., Sect. A **447**, 218 (2000).
 - [8] L. Balka *et al.*, Nucl. Instrum. Methods Phys. Res., Sect. A **267**, 272 (1988).
 - [9] S. Bertolucci *et al.*, Nucl. Instrum. Methods Phys. Res., Sect. A **267**, 301 (1988).
 - [10] R. Oishi, Nucl. Instrum. Methods Phys. Res., Sect. A **453**, 227 (2000); M.G. Albrow *et al.*, Nucl. Instrum. Methods Phys. Res., Sect. A **480**, 524 (2002).
 - [11] F. Abe *et al.* (CDF Collaboration), Phys. Rev. D **45**, 1448 (1992).
 - [12] A. Bhatti *et al.*, Nucl. Instrum. Methods Phys. Res., Sect. A **566**, 375 (2006).
 - [13] D. Acosta *et al.* (CDF Collaboration), Phys. Rev. D **71**, 052003 (2005).
 - [14] T. Sjostrand *et al.*, J. High Energy Phys. **05** (2006) 026.
 - [15] H.L. Lai *et al.*, Eur. Phys. J. C **12**, 375 (2000).
 - [16] R. Field, AIP Conf. Proc. **828**, 163 (2006).
 - [17] F. Abe *et al.* (CDF Collaboration), Phys. Rev. D **48**, 2998

(1993).

- [18] D. Acosta *et al.* (CDF Collaboration), Phys. Rev. Lett. **95**, 022003 (2005).
- [19] A. Abulencia *et al.* (CDF Collaboration), Phys. Rev. D **74**, 032008 (2006).
- [20] S. Klimenko, J. Konigsberg, and T. M. Liss, FERMILAB Report No. FN-0741, 2003.
- [21] P. M. Nadolsky, Phys. Rev. D **78**, 013004 (2008).